NATIONAL RADIO ASTRONOMY OBSERVATORY
SOCORRO, NEW MEXICO

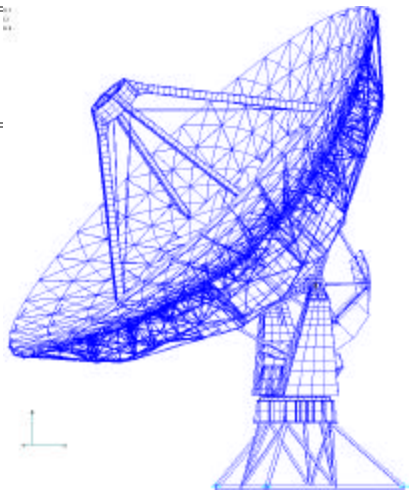

VLA TEST MEMO # 220

# PHOTOGRAMMETRIC MEASUREMENT OF VLA AND VLBA SUBREFLECTORS AND VLA PRIMARY REFLECTOR

APRIL 26, 1999

**B. BUTLER, J. RUFF, J. THUNBORG**

## 1.0 BACKGROUND

The measurement of the surfaces of the VLBA antennas presents particular challenges when trying to reach the desired measurement accuracy (Butler 1998). Indirect methods (microwave holography, for instance) have been unable to achieve the desired accuracy and reliability. Older direct methods (theodolite and tape, for instance) have associated problems which make them undesirable in general. However, a more modern direct technique for measuring antenna surfaces may actually serve NRAO very well in terms of accuracy, ease of use, portability, and reliability. This technique is "photogrammetry". In this technique, optical photographs are taken of a surface which has been prepared with retroreflective targets, and then used to derive the absolute spatial locations of the targets (and hence of the surface). This technique is described in Fraser (1986) and Fraser (1993). In particular, digital photogrammetry, which involves the use of a CCD rather than photographic film, seems attractive because of the portability of the system and the quick turnaround on processing. Reported accuracies for this type of system are in the range of 1:100000 to 1:250000, where the accuracy is a ratio of the linear size of the object to be measured. For the 25 meter main reflector surfaces of the VLBA antennas, this might yield accuracy as good as (or better than) 250 μm. For the roughly 3 meter VLBA subreflectors, the accuracy may be as good as (or better than) 30 μm. For some time now, we have been considering the purchase of a photogrammetry system, but we wanted to have a demonstration of its use. This demonstration would allow us to gauge for ourselves how easy to use and portable such a system would be, and allow us to test the true accuracy of such a system for the particular application of measuring a large radio antenna reflector and subreflector. This memo describes such a demonstration and the results of the analysis of the resultant derived reflector and subreflector geometries. In addition, an analysis of the gravitational deflection of a VLA antenna is presented.

## 2.0 DESCRIPTION OF THE TEST

The recognized industry leader in the manufacture of photogrammetric systems is Geodetic Services, Inc. (GSI), in Melbourne, Florida. We arranged with John Brown, the president of GSI, for a demonstration of a digital photogrammetric system at the VLA. We decided that it was more desirable to measure a VLA antenna than a VLBA antenna, because we might be able to compare the derived surface profiles with "ground truth" from holography experiments (Rick Perley has been doing these for some time now). In fact, this type of analysis requires a combination of the absolute geometries of the main reflector and subreflector, and we have not conducted such an analysis yet (though we hope to in the future). We decided that measurements of the VLA antenna in 3 geometries were desirable.

One of the advantages of a photogrammetric system is the ability to measure the antenna surface at a variety of elevation angles, and we wanted to test this. We decided that measurements with the antenna pointed to horizon, zenith, and 45 deg would be undertaken. Repeatability tests would be performed, concentrating on the 45 deg setting. The VLA subreflector would be measured, and a repeatability test performed. In addition, the spare VLBA subreflector (which sits in the AAB) would be measured, and repeatability tests performed. The tests were performed on November 19 and 20, 1998, by John Brown. A very good description of the tests themselves was written up by John Brown (Brown 1998). We decided to measure the antenna in the AAB (antenna 13) in order to reduce possible inclement weather effects. We worried about differential temperature effects in the barn, so did the bulk of the main reflector measurements at night (more than an hour after sunset) in order to mitigate these effects.

## 3.0 EQUIPMENT

The V-STARS camera system (manufactured by GSI) is a 3-D coordinate measurement system based on photogrammetry. The V-STARS system uses the hand held high resolution digital camera shown in Figure 1 (the INCA camera) and a notebook computer to triangulate the 3-dimensional positions of retro-reflective targets placed on the measured object. The camera is used to take pictures from several geometrically diverse locations to get intersection points for triangulation. These data (pictures) are then processed in the laptop computer and the 3-dimensional coordinates of the targets with respect to an arbitrary coordinate system are then determined. The entire system is very portable, and can be taken on normal airline travel. The three main components of this system are the camera, the targets, and the laptop, which will each be discussed in more detail now.

Figure 1. The INCA camera.

### 3.1 CAMERA

The INCA camera weighs approximately 8 pounds, which means that it can be easily operated by a single person. The camera has several lenses and flashes, and it became apparent during the tests that some familiarity with these items will be necessary for the operator of the system. Different combinations of lens and flash are required to obtain the best results under different illumination and geometry conditions. The camera has an attached CCD (3K horizontal X 2K vertical), which is in turn attached to an incorporated microprocessor. It has its own intelligence, and can be programmed via a somewhat crude interface (reminiscent of a printer). A removable laptop disk is inserted into the camera, and when all of the pictures for a particular "job" have been taken, the disk is removed from the camera and inserted into the laptop. Capacity of these disks was of order several hundred Mb.

### 3.2 TARGETS

The retroreflective targets are printed on black adhesive backing tape and were relatively easy to handle. They came in two sizes: larger ones for the main reflector (1" diameter for the retroreflective portion), and smaller ones for the subreflectors (0.25" diameter). The larger ones came on a roll, with 1.5" separation and 1200 total targets on the roll. The cost for this roll is about $220. The smaller ones came on a sheet, with 150 targets on the sheet. Cost for this sheet is about $35. The smaller ones had an alternate type, where they were spaced much more densely on a roll (0.2" targets – 1800 to a roll - $80 per roll). These were used on the primary axes of the VLBA subreflector. Target thickness is 122 +/- 5 μm for all of the targets. Targets were placed on the VLA subreflector with about 6" spacing (3" on the two axes – 260 targets total), and on the VLBA subreflector with about 6" spacing (1" on the axes – 602 targets total). They were

initially placed on the VLA main reflector at the corners of all of the panels. When John Brown arrived at the site on 19Nov, he pointed out that the reflectors were too close, and we had to retarget the main reflector. While doing this, we added another target in the center of each panel. This gave us 860 total targets on the main reflector surface. The retargeting took about 2 hours for 4 of us. Getting the retroflector tape to adhere to the main reflector surface was not straightforward, and we will need to work on this procedure if we want to use this system.

A second type of retroreflective target is required in order to do the triangulation properly. This type of target is called a "code" target. These targets are square, and have a hard backing to them. They have special patterns which are recognized by the software in order to aid in finding target locations. For the main reflector surface, 48 code targets of about 10 cm size (on a side) were used. For the VLA subreflector, 24 code targets were used, and for the VLBA subreflector, 16 code targets were used (both about 4 cm on a side).

In order to fix the absolute geometry of the targets (as opposed to strictly relative geometry), two final types of targets are required: the "scale bar" and the "auto bar". The scale bar is simply a connectable set of bars of accurately measured length, with retroreflective targets on both ends. We had 3 such bars (which could be connected together), labeled A, B, and C. For the main reflector, we connected all 3 of these together, and attached them to the surface. For the subreflectors, we used them separately, on different parts of the surface. The auto bar is a target of easily recognizable shape (by the software) which also has known absolute dimensions. In our tests, the auto bars were in the shapes of crosses. In order to fix the scale bars and auto bars to the surfaces, hot melt glue was used. Initially, we used simple bent cardboard for this attachment. We quickly learned that a something better was needed (when the auto bar and scale bars came loose from the main reflector!). Small blocks of wood with angled bottoms worked very well.

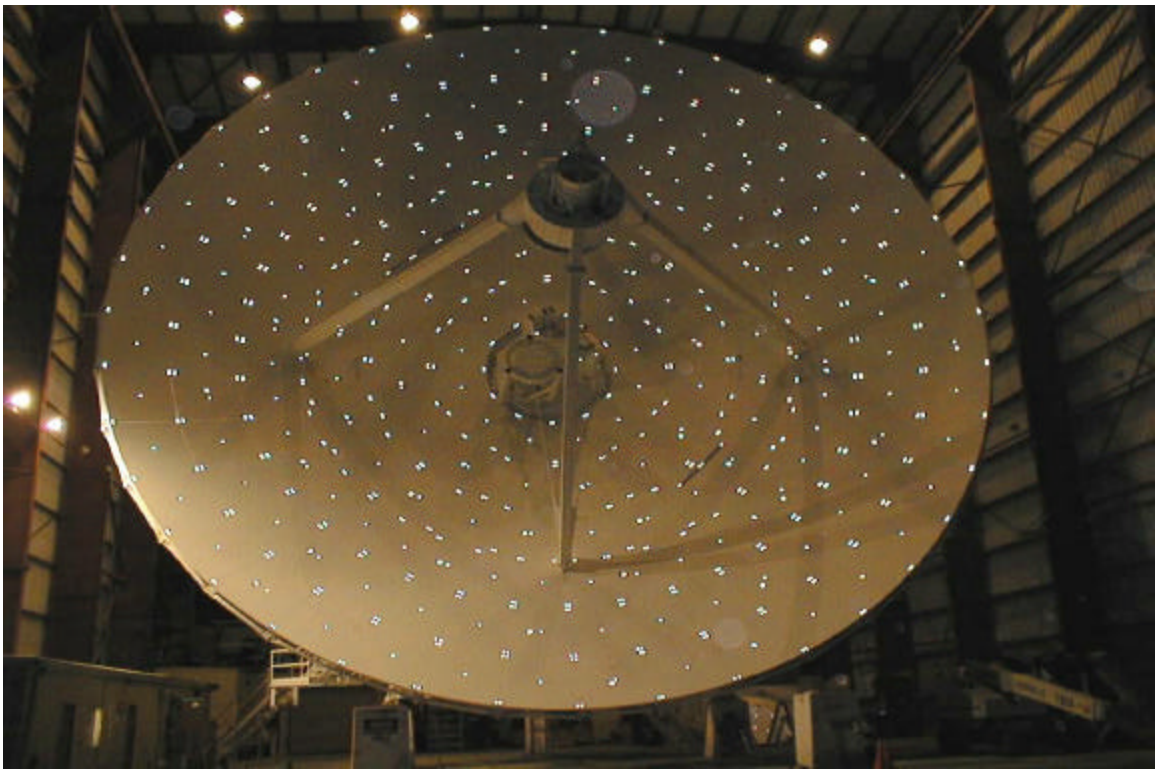

Figure 2. VLA Primary Reflector Photogrammetry Targets.

Figure 2 shows the VLA antenna with all attached targets, and Figure 3 shows the VLBA subreflector with all attached targets. It took approximately 20 person hours to target the main reflector surface and two subreflector surfaces.

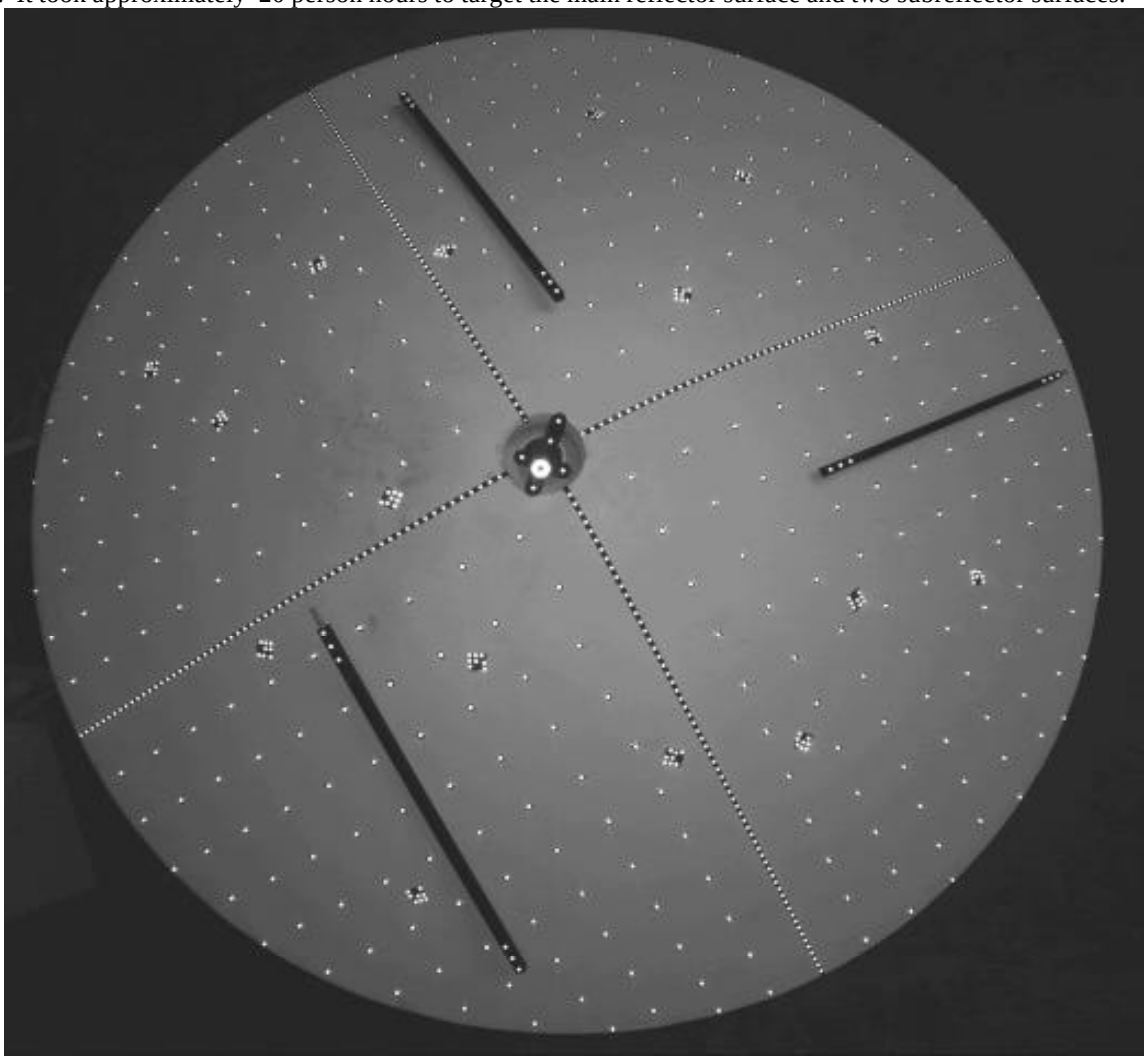

Figure 3. VLBA Subreflector Photogrammetry Targets.

3.3 LAPTOP/SOFTWARE

As mentioned above, when all pictures for a given orientation/geometry were taken, the removable disk was taken from the camera and inserted into the laptop. The laptop is supplied with the V-STARS system. There is a discount if we want to purchase our own laptop to use with the system, but in this case, there is no guarantee from GSI that their software will work. The laptop was running standard Windows95. GSI has an extensive software suite which is used to process the data, and it is quite complicated. The process was very quick for John Brown, but it was clear that he was a black-belt at this process. We suspect that the learning curve for the software is quite steep, and we would have to be willing to spend the time/money to have operators of the system properly trained in its use. The software is used to do all of the steps necessary to obtain a final set of cartesian coordinates (x,y,z triples) for all of the targets, including the auto bar, the scale bars, the code targets, and the standard targets. The end product of this processing is an ASCII file

containing target identifiers and associated x,y,z triples. For more details on the processing steps (e.g. initial triangulation, bundle adjustment, etc…) please refer to the GSI documentation or the literature.

3.4 CRANES ETC…

In order to get the camera and operator (John Brown) into the proper position to take the photographs, it was necessary to use both of the cranes at the VLA site. The small crane (T-Rex) was used in the photographing of the VLBA subreflector (when a crane was needed – many of these photos were taken from the ground or from a ladder). The T-Rex was also used during the photographing of the VLA subreflector (the antenna was tipped to horizon, and the lift arm was extended through the quadropod legs). The larger crane (the man-lift) was used (with attached extension jib) for all of the main reflector photographing.

As mentioned above, we were worried about differential temperature effects in the barn, so we had a digital thermometer in the barn to test when the temperature became stable after sunset. In the future, more careful temperature measurements should probably be done, but we felt that the increased effort was unwarranted for this initial test.

## 4.0 MEASUREMENT CONDITIONS AND INTERNAL CONSISTENCY ACCURACY ESTIMATES

In total, 11 separate measurements were made on the primary reflector of VLA antenna, 2 on the subreflector of that antenna, and 3 on the VLBA subreflector. The conditions of each measurement are described in Table 1. A more detailed explanation of each measurement is available in Brown (1998). A byproduct of the processing to locate the positions of the targets is an accuracy estimate of the locations in the three coordinate directions. This is essentially an internal consistency estimate from the best fit solution for each target location (similar to the SNR from a self-calibration solution). These internal accuracy estimates are shown in Table 1 for the 3 coordinate axis directions. For us, the Z-axis was along the line from the center of the main reflector up to the center of the subreflector (along the optical axis), the X-axis pointed almost along the direction of the elevation axis, and the Y-axis was orthogonal (akin to the azimuth direction). So, for our purposes, the accuracy of the Z direction is the one of more interest, because it is more closely related to the accuracy with which the surface irregularities can be measured. It is clear from this table that the accuracy estimate from the internal consistency is in almost all cases better than our desired 100 μm (Butler 1998). The daytime measurements are worse, but it is clear that if we used such a system, it would be used at night, when conditions are most stable.

## 5.0 REPEATABILITY TESTS

A check of the internal accuracy estimates is to compare measurements against each other by differencing the derived positions of the targets from two different measurements, and taking the RMS of these differences. Table 2 shows the results of some of these comparisons (not all measurements are intercompared, only those with some meaning). These numbers are similar to the ones from the internally derived accuracy, lending some amount of believability to them. Note that in almost all the main reflector cases, the RMS of the difference is near the accuracy that we desire (100 μm), and in the most careful of the measurements, it surpasses this goal (as good as 70 μm on the main reflector). In the subreflector repeatability cases, the desired measurement accuracy (of order 30 μm) is reached for all of the measurements. We will now examine some of these repeatability tests in more detail.

**Table 1 - Summary of measurement conditions and internally estimated accuracy.**

| # | Description. | Accuracy Estimate mm | | | Conditions | Date |
|---|---|---|---|---|---|---|
| | | X | Y | Z | | |
| 1 | Reflector at zenith (even numbered pictures). Antenna moving in Azimuth, Camera stationary. Pictures for measurements 1 and 2 were taken during the same time period. | 53 | 53 | 76 | Night, Stable Temperature | 11/19/98 |
| 2 | Reflector at zenith (odd numbered pictures) Antenna moving in Azimuth, Camera stationary. | 56 | 61 | 76 | Night, Stable Temperature | 11/19/98 |
| 3 | Reflector at 45 degrees, Antenna stationary camera moved to less than ideal geometric positions. | 46 | 51 | 74 | Night, Stable Temperature | 11/19/98 |
| 4 | Reflector at 45 degrees (4 panels moved) Antenna stationary camera moved to less than ideal geometric positions. | 76 | 74 | 114 | Night, Stable Temperature | 11/19/98 |
| 5 | Reflector at horizon (4 panels moved) | 76 | 76 | 102 | Night, Stable Temperature | 11/19/98 |
| 6 | Reflector at 45 degrees, Improved Camera geometry. Picture sets for measurements 6 and 7 were taken together. | 99 | 102 | 137 | Daytime | 11/20/98 |
| 7 | Reflector at 45 degrees Improved Camera geometry. | 102 | 102 | 140 | Daytime | 11/20/98 |
| 8 | Reflector at 45 degrees Improved Camera geometry. Picture sets for measurements 8 and 9 were taken together. | 61 | 64 | 86 | Night, Stable Temperature | 11/20/98 |
| 9 | Reflector at 45 degrees Improved Camera geometry. | 56 | 61 | 81 | Night, Stable Temperature | 11/20/98 |
| 10 | Reflector at 45 degrees (4 panels moved) Improved Camera geometry. | 61 | 64 | 89 | Night, Stable Temperature | 11/20/98 |
| 11 | Reflector at 45 degrees (4 panels moved) Improved Camera geometry. Repeat of measurement 10 without moving the antenna. | 56 | 61 | 81 | Night, Stable Temperature | 11/20/98 |
| 12 | VLBA Subreflector (Moving camera around subreflector) | 13 | 13 | 20 | Day | 11/19/98 |
| 13 | VLBA Subreflector (Moving camera around subreflector) | 18 | 18 | 23 | Day | 11/19/98 |
| 14 | VLBA Subreflector (Rotating Subreflector around fixture with camera in same location) | 18 | 18 | 25 | Day | 11/19/98 |
| 15 | VLA Subreflector on antenna 13 | 10 | 10 | 15 | Day | 11/19/98 |
| 16 | VLA Subreflector on antenna 13 | 10 | 10 | 15 | Day | 11/19/98 |

**Table 2 - Summary of repeatability/differencing tests.**

| Differenced measurements | Description | RMS of difference (mm) X | Y | Z |
|---|---|---|---|---|
| 8 & 9 | Friday night, same time and conditions | 83.8 | 81.3 | 68.6 |
| 10 & 9 | First measurement after adjusting | 172.7 | 157.5 | 124.5 |
| 11 & 9 | Second measurement after adjusting | 106.7 | 114.3 | 94.0 |
| 10 & 11 | First vs second measurement after adjusting | 185.4 | 116.8 | 76.2 |
| 3 & 4 | Thursday night, before vs after adjusting | 147.3 | 114.3 | 177.8 |
| 3 & 9 | Friday night vs Thursday night before adjusting | 104.1 | 106.7 | 109.2 |
| 4 & 9 | Friday night vs Thursday night after adjusting | 162.6 | 157.5 | 188.0 |
| 6 & 7 | Friday daytime, same time and conditions | 132.1 | 134.6 | 106.7 |
| 15 & 16 | VLA subreflector | 7.5 | 7.7 | 13.9 |
| 12 & 13 | VLBA subreflector | 17.9 | 19.1 | 23.4 |
| 12 & 14 | VLBA subreflector | 19.9 | 16.9 | 21.9 |
| 13 & 14 | VLBA subreflector | 24.1 | 21.1 | 24.6 |

The best case in the repeatability experiments were the measurements done on 20Nov (camera positioning was superior for those measurements). The comparison of measurements 10 and 11 (done at 45 deg) were nearly ideal, as the antenna had panels in their original (unmoved) positions (see 'panel movement' section below). The only change between these two measurements was a small (3 deg F) temperature decrease between the first and second measurements. Figure 4 shows the differenced normal to the surface for these two data sets. The standard deviation over the entire main reflector surface was 63 μm. This agrees quite well with the internal accuracy estimate, and the raw Z-axis difference rms. Note, however, that the error pattern shown in Figure 5 is not entirely random – it has a slight "potato chip" appearance.

Figure 4. Difference between measurements 10 and 11. Color scale is in mm.

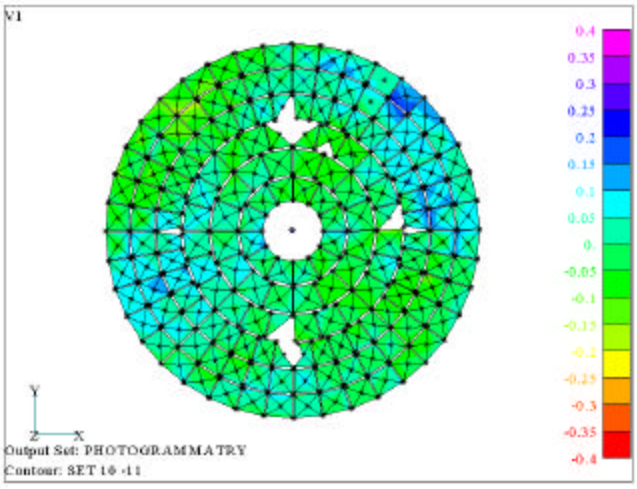

When the structure was measured at 45 degrees, moved to zenith, then back to 45 degrees where it was measured again, the measurements did not repeat as well as when the structure was not moved. If we look at the unmoved panels in data set 10 and compare them to the unmoved panels in data set 9, we find the RMS repeatability is 106 μm. The contour plot of the difference normal to the reflector surface for sets 9 and 10 is shown in Figure 5. Figure 6 shows the comparison between the Thursday night (set 4) and Friday night (set 10) data. The RMS of the difference normal to the surface between these two measurements is 133 μm, i.e., it gets worse as the amount of time between the two measurements (and the amount of movement) is increased.

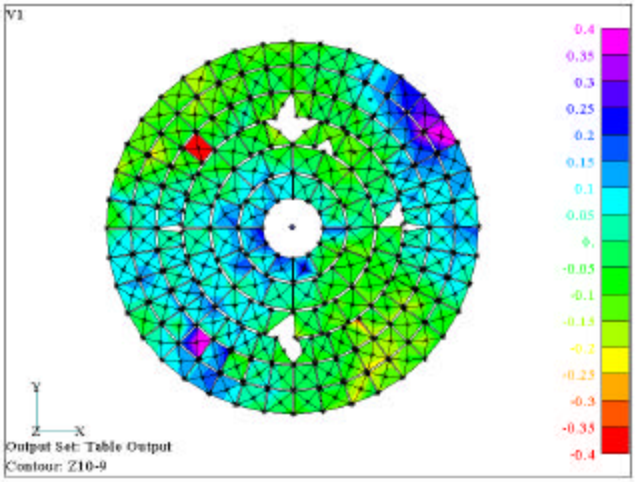


Figure 5. Difference between measurements 9 and 10. Color scale is in mm.

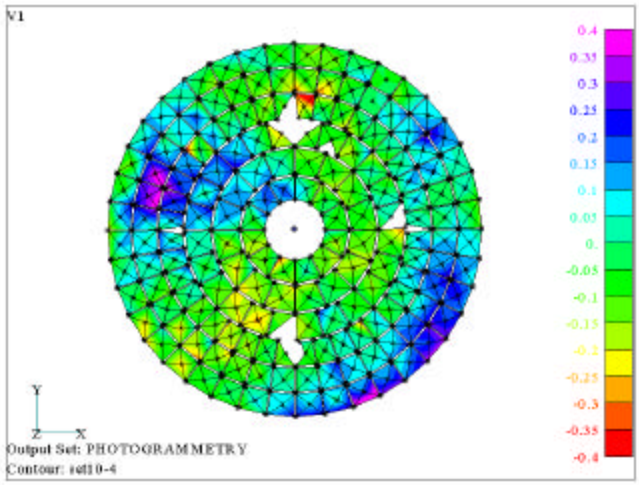


Figure 6. Comparison of Thursday and Friday night measurements. Color scale is in mm.

## 6.0 ACCURACY TESTS FROM PANEL DISPLACEMENT

In an effort to determine what the absolute accuracy of the surface determination was for the photogrammetry system, we made measurements before and after displacing 4 panels by a known amount, and compared the resultant differences in the derived panel positions to the known displacement amounts. Measurements 9 and 10 were the before and after panel displacement tests. For the unmoved panels, the RMS difference in the surface normal direction for the two measurements was 106 μm. Figure 7 shows which panels were moved on a cartoon of the main reflector surface, and the measured displacement normal to the antenna surface for the two measurements. Panel 1 was displaced -800 μm, panel 2 was displaced +400 μm, panel 3 was displaced -200 μm, and panel 4 was displaced +100 μm (as indicated in Figure 8).

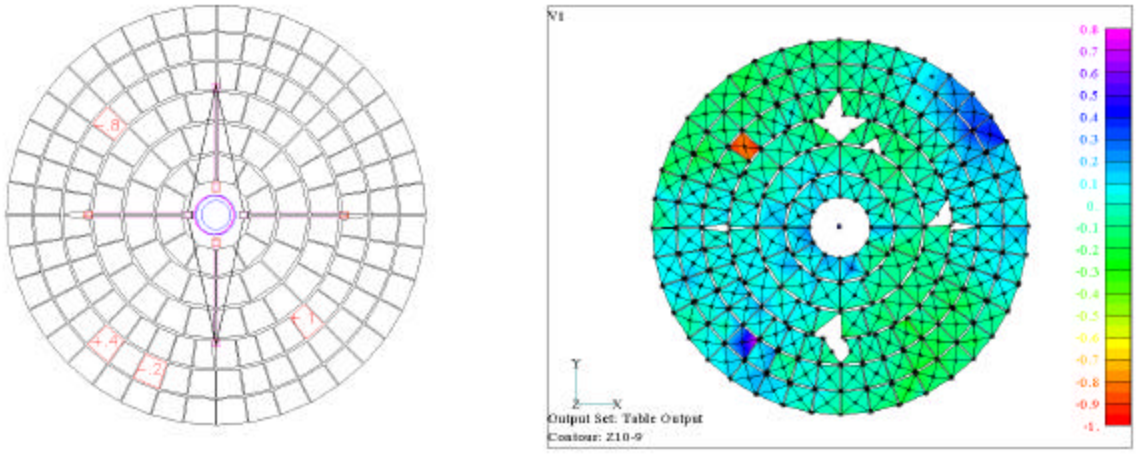


Figure 7. Moved panels and measured displacement. Color scale in right hand panel is in mm.

**Table 3. Moved panel statistics.**

.

| Location | Panel 1 (-.813) | Error μm | Panel 2 (+.406) | Error μm | Panel 3 (-.203) | Error μm | Panel 4 (+.102) | Error μm |
|---|---|---|---|---|---|---|---|---|
| Corner 1 | -.795 | +48 | +.309 | -97 | -.051 | +152 | -.233 | +355 |
| Corner 2 | -.946 | -133 | +.110 | -296 | +.018 | +221 | -.140 | +242 |
| Corner 3 | -.778 | +17 | +.185 | -221 | +.101 | +304 | +.003 | +99 |
| Corner 4 | -.922 | -109 | +.769 | +363 | +.130 | +.333 | -.145 | +247 |
| Center | -.812 | +1 | +.402 | -4 | +.008 | +211 | -.099 | +201 |
| Average | -.851 | -38 | +.355 | -51 | +.038 | +.241 | -.123 | +225 |
| RMS | | 80 | | 235 | | 253 | | 243 |

Table 3 shows the resultant statistics on the moved panel measurements. The average 1σ RMS total error is 203 μm. However, there is uncertainty in the repeatability of the structure itself. There is also some uncertainty in how far the panels were moved. We estimate our panel setting to be accurate to approximately 100 μm. The total RMS error for the unmoved panels was 106 μm. From the repeatability test described in section 5.0, we know that without moving the structure the camera is repeatable to 63 μm. Assuming that the total error for the unmoved panels is the RSS of the structure error and the camera error gives for the structural repeatability error:

$$s_{structure} = \sqrt{s^2_{unmoved} - s^2_{camera}} = \sqrt{106^2 - 63^2} = 85\,mm$$

Then the absolute accuracy for the moved panels is given by the absolute error less the structural repeatability error and the panel setting error:

$$s_{accuracy} = \sqrt{s^2_{total} - s^2_{structure} - s^2_{setting}} = \sqrt{203^2 - 85^2 - 100^2} = 155\,mm$$

For the 25-meter VLA dish, this gives us a 1σ absolute accuracy of 6.2 ppm (or about a 160000:1 measurement). This accuracy is very close to the accuracy found in a very detailed Boeing acceptance test (Brown 1997) where the V-STARS system was compared to a laser tracker. The Z-Axis accuracy for a low aspect ratio object was found to be 8.5 ppm. Boeing also conducted a test on a high aspect ratio object whose length was 10 times its width. The accuracy of this measurement was 3 ppm.

## 7.0 DEVIATION FROM IDEAL SURFACE AND GRAVITATIONAL DEFORMATION

### 7.1 VLA Primary Reflector

#### 7.1.1 Deviation from ideal surface

The shape of the VLA primary reflector approximates a paraboloid, but deviates to a minor extent in order to improve its performance. The exact shape of this surface is described in the VLA Panel Specification (see Wilkinson reference below). This document lists the Z-axis height of the surface in terms of the radius in one-inch increments for the entire surface. A 12$^{th}$ degree polynomial curve fit of this data was used to generate a numerical model of the dish surface. The residuals from the curve fit were less than 13 μm. The measured dish shape was then compared with the curve fit data using a Mathcad program. A contour plot of the distance normal to the dish between the specified surface and measured surface is shown in Figure 8.

The panel positions on this antenna were optimized using holography. However, the contour plot clearly shows a 4 mm hump on the upper left part of the dish and a 2mm depression on the lower right. The measured shape of the dish indicates that the holography was compensating for other systematic effects such as subreflector shape or location. A complete ray trace of both the dish data and the subreflector data is required to completely understand why the panel positions deviate so far from the theoretical optimum. We are in the process of attempting to perform this ray trace, but have not completed that part of the analysis to this point.

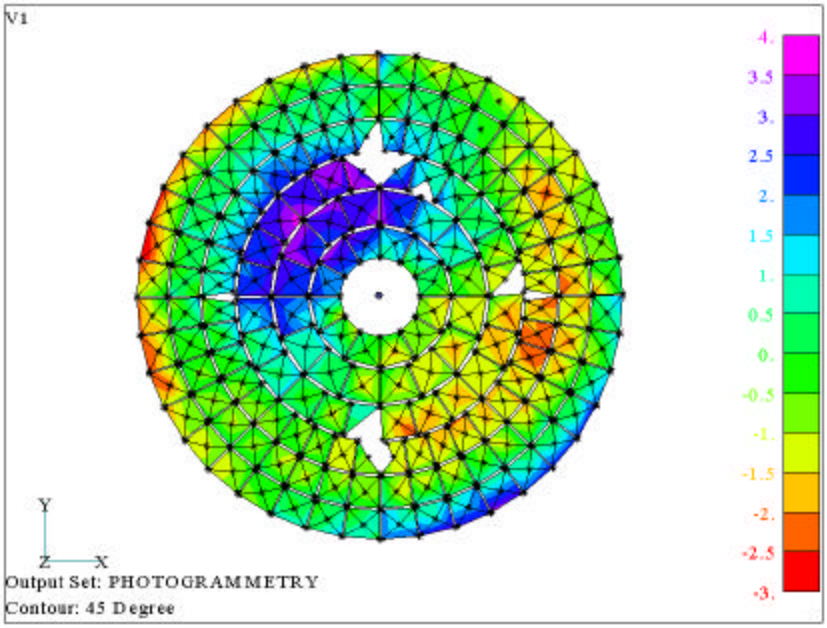


Figure 8. Difference between measured surface for VLA antenna 13 and the ideal surface. Blank portions of the image represent targets that were shielded by the quadropod legs. Color scale is in mm.

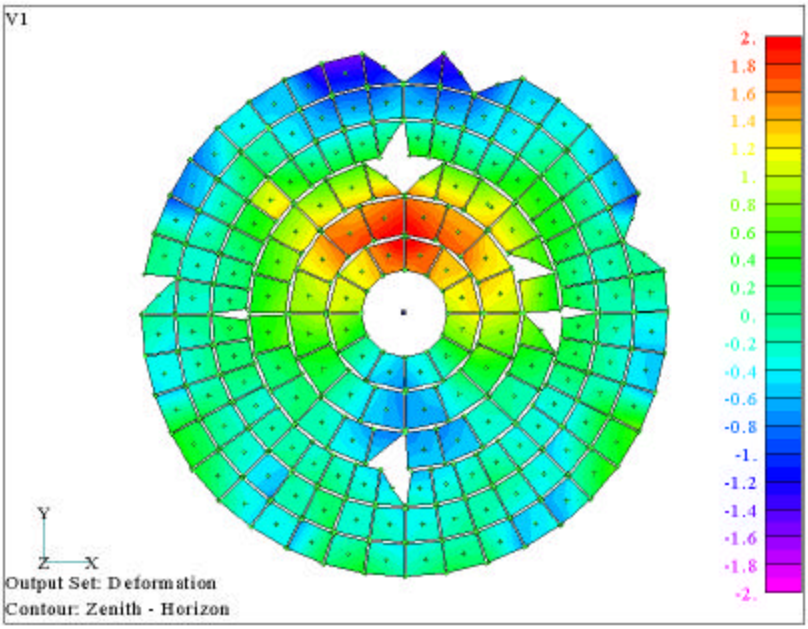


Figure 9. Gravitational deformation normal to surface of primary reflector. Zenith minus Horizon pointing.

7.1.2 Gravitational deformation

Since the photogrammetry could easily be repeated at different dish elevations, it was used to measure the gravitational deformation of the antenna. Figure 9 shows the difference normal to the surface in the dish shape due to gravitational sag between the zenith position and the horizon. The standard deviation of the difference is 0.67 mm. This difference map corresponds extremely well with what is predicted using a structural model of the VLA antennas (J. Thunborg., in preparation).

7.2 VLA and VLBA Subreflectors

## 7.2.1 VLA subreflector deviation from ideal shape

For the VLA subreflector, Peter Napier's MathCad worksheet (vlamain.mcd) was used to generate a table of theoretical Z dimensions on a 1 inch grid in X and Y. The theoretical dimensions were interpolated to photogrammetry points using the following formula:

$$\mathbf{Z = C_1 + C_2x + C_3x^2 + C_4y + C_5y^2}$$

For each photogrammetry target location, the closest theoretical point was located. That point, with the four points at (x ± 1, y) and (x, y ± 1) were used to solve for **C**. The interpolation was tested by predicting Z for (x + 1, y + 1) and found to be in agreement with the tabulated data within 25 μm. For points near the edge, the interpolation was shifted to place all interpolation points within the defined subreflector. Because of this, edge points may have a slightly larger error.

Using known positions of four points, the photogrammetry data set was rotated and translated to place it near the theoretical data. The sum of errors squared $\mathbf{(Z_{theoretical} - Z_{photogrammetry})^2}$ was computed. Translations and rotations were then adjusted manually to minimize the sum of errors squared. This method works, but it must be used with caution because there are many local minima in the error squared function. If you don't start from a point close to the best fit location, the method may converge to a wrong solution.

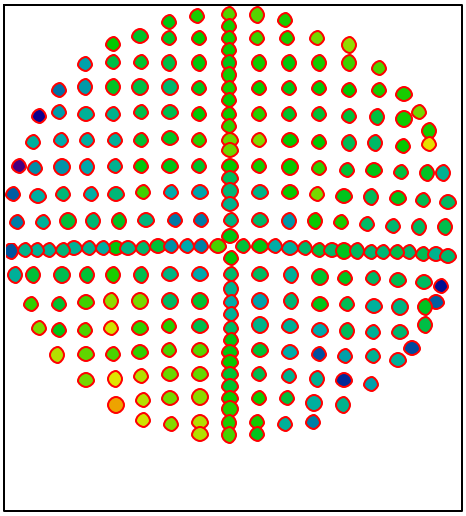

SRPG<0>, SRPG<1>, Error
Individual PG Point Errors: Top view

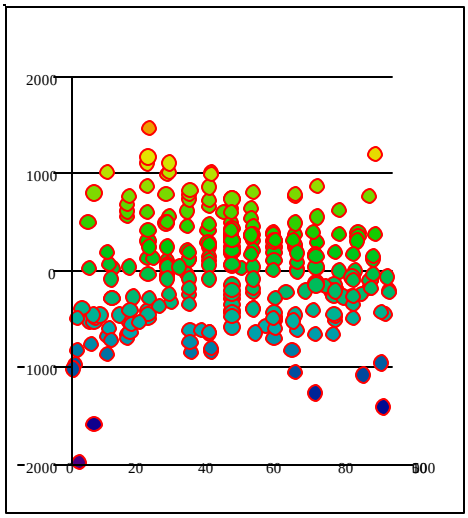


SRPG<0>, SRPG<1>, Error·25400
Individual PG Point Errors: Side view

Figure 10. VLA Subreflector shape error. Left-hand panel shows errors vs. x/y coordinates at each of the target locations. Right-hand panel shows error vs. position along the Y axis (parallel to axis of symmetry).

For the VLA subreflector, the best fit RMS error was 533 µm with the maximum error of 1.98 mm. The magnitude and position of the error on the surface is shown in Figure 10. This error is Z-axis error, not surface normal error.

### 7.2.2 VLBA subreflector deviation from ideal shape

The VLBA subreflector geometry is defined in a table, with Z dimensions given on one inch spacings in X and Y. (File name VLBASR.dat). The theoretical dimensions were interpolated to photogrammetry points using the identical algorithm used on the VLA subreflector.

For the VLBA subreflector, we found a best fit of 305 µm RMS with 1.52 mm maximum error using photogrammetry data set 12. Data set 13 yielded practically identical results. Ignoring points beyond 1.5 meter radius, the RMS drops to 229 µm with 813 µm maximum error.

As evidenced in Figure 11, the VLBA subreflector errors are radius dependent, with high readings at the edges and center surrounding low readings in a 1 meter radius ring - corresponding approximately to the mounting structure.

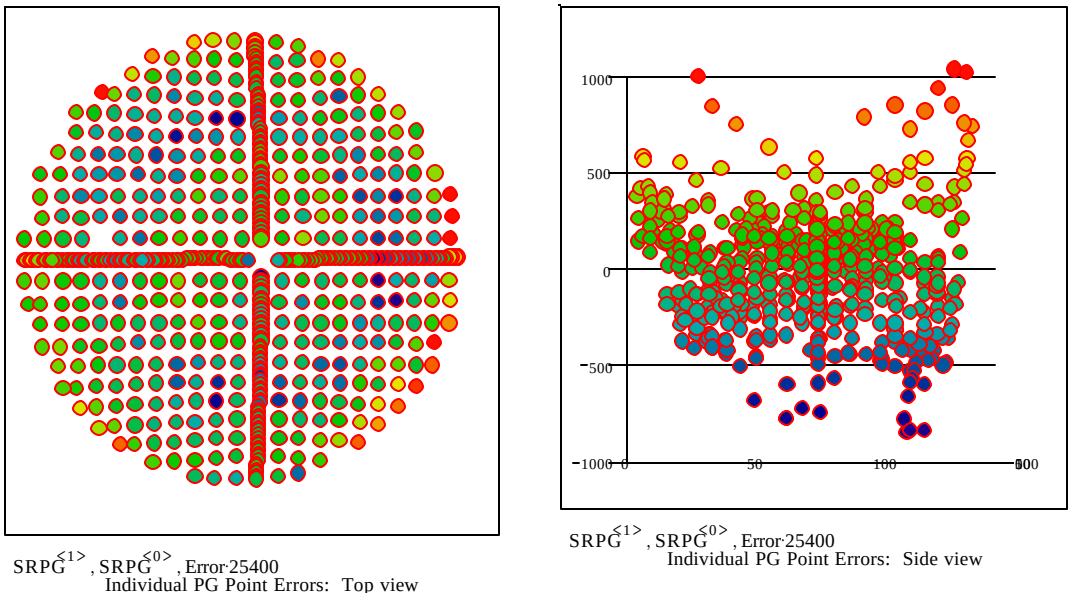


Figure 11. VLBA Subreflector shape error. Left-hand panel shows errors vs. x/y coordinates at each of the target locations. Right-hand panel shows error vs. position along the X axis (parallel to axis of symmetry).

This radial dependence of the error is displayed in Figure 12, which shows the errors as a function of distance from the geometrical center of the VLBA subreflector. The low points around the radius of the mounting structure are very easily seen.

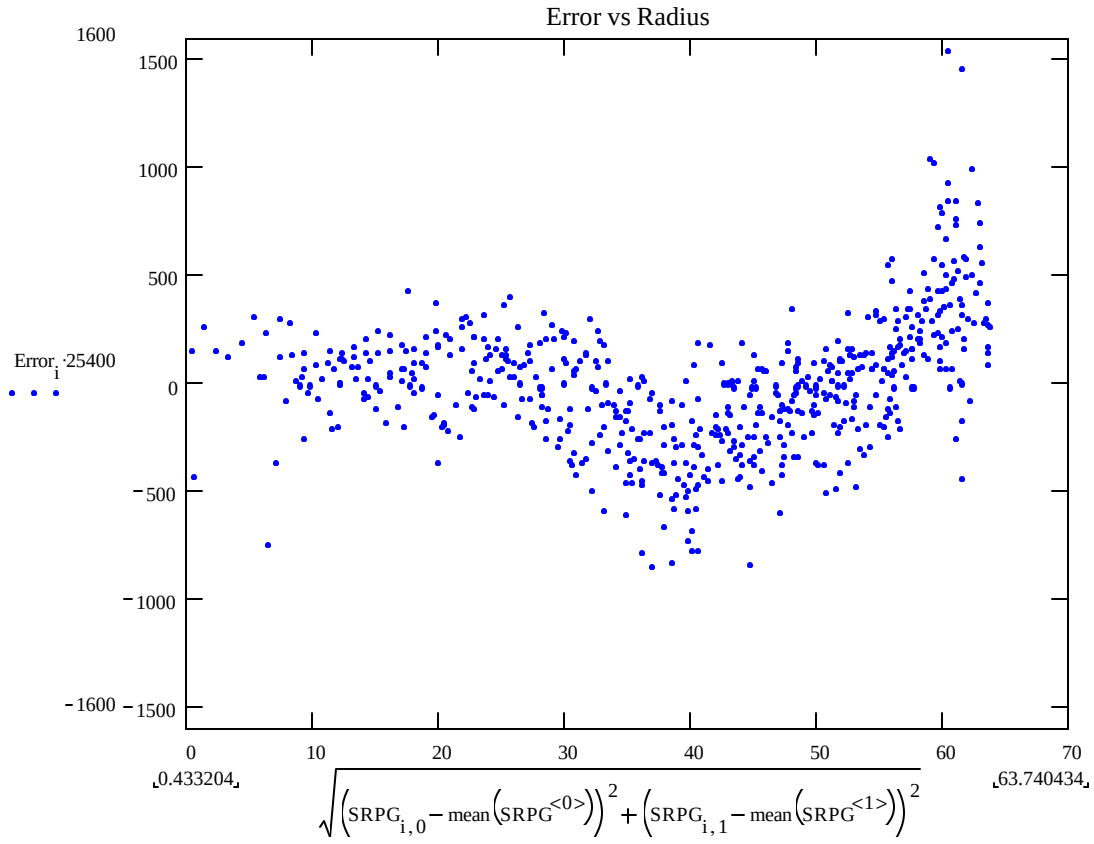


Figure 13. Deviation from ideal surface for the VLBA subreflector. Errors are plotted as a function of distance from the geometric center of the subreflector – scale is +/- 1600 μm.

## 8.0 SUMMARY AND CONCLUSIONS

From this demonstration, the indications are that photogrammetry is a very useful tool for measuring both subreflectors and primary reflectors. It can give very accurate results with very little setup time. Repeatability accuracy as good as 65 μm was demonstrated on the VLA primary reflector surface. Absolute accuracy may be twice as bad, but a more controlled test probably needs to be performed to determine this well. Repeatability accuracy was as good as 14 μm on the VLA subreflector, and 22 μm on the VLBA subreflector. All of these repeatability accuracies are well within the desired measurement accuracy for the VLBA primary reflector and subreflector.

Subreflector repair could be accomplished using photogrammetry but it may be tedious, as the subreflector might have to be retargeted for each measurement during the repair process. This would be a very good way of acceptance testing any subreflectors we buy in the future, however.

**ACKNOWLEDGEMENTS**

Thanks to Ramon Gutierrez, Martin Lopez, Ramon Molina, and Gilbert Montano who worked well into the night operating the crane and moving panels in subfreezing temperatures.

**REFERENCES**

Brown J., Boeing Acceptance Test Results, GSI internal report, 1997

Brown, J., Report of V-STARS Demonstration Measurement at NRAO, GSI internal report, 1998

Fraser, C.S., Microwave antenna measurement by photogrammetry, *Photogramm. Eng. Rem. Sens. 58,* 305-310, 1986

Fraser, C.S., A resume of some industrial applications of photogrammetry, *J. Photogramm. Rem. Sens., 48,* 12-23, 1993

Wilkinson J.W., VLA Panel Specification for an 82-foot Diameter Radio Telescope, E-Systems Garland Division, NO. 96S20206.